Construction and Building Materials 525 (2026) 146355

Contents lists available at ScienceDirect

Construction and Building Materials

journal homepage: www.elsevier.com/locate/conbuildmat

Enhancing the fire resistance and fungal durability of solid wood *via* magnesium carbonate-based mineralization method

Andreja Pondelak [a,*], Nataša Knez [a], Srečo Davor Škapin [b], Miha Humar [c], Andrijana Sever Škapin [a,d,**]

[a] Slovenian National Building and Civil Engineering Institute, Dimičeva ulica 12, Ljubljana 1000, Slovenia
[b] Jožef Stefan Institute, Jamova 39, Ljubljana 1000, Slovenia
[c] University of Ljubljana, Biotechnical Faculty, Jamnikarjeva 101, Ljubljana 1000, Slovenia
[d] Faculty of Polymer Technology – FTPO, Ozare 19, Slovenj Gradec 2380, Slovenia

ARTICLE INFO

Keywords:
Mineralization
$MgCO_3$
Reaction to fire
Fungal durability
Environmentally friendly

ABSTRACT

Enhanced fire performance and durability of wood materials and products without harmful chemicals remains an important challenge. We propose a specific magnesium carbonate-based mineralization method for improving wood durability and fire resistance. During mineralization wood samples were impregnated with an aqueous solution of magnesium acetoacetate, which subsequently transforms within the wood to form various magnesium carbonate-based compounds, predominantly different hydrated and basic phases, the specific formation of which is influenced by factors such as wood anatomy and environmental conditions during post-treatment. Unlike traditional calcium carbonate, magnesium carbonates decompose at much lower temperatures, releasing both water and CO_2, which together contribute to enhanced flame protection through cooling and dilution of flammable gases. This treatment delayed ignition time by over 50% in two case studies, Norway spruce and European beech, compared to untreated controls. Additionally, such mineral-wood composites showed significantly lower mass loss when exposed to fungi, attributed to increased alkalinity compared to the untreated wood's acidity. This dual-function mineralization approach offers an environmentally friendly alternative for improving fire and decay resistance and presents a non-hazardous biocide-free method that could replace certain conventional treatments.

1. Introduction

Due to its excellent properties, and the biological origin, wood finds applications across a wide range of industries. However, its use, particularly in construction, is challenged by its low resistance to burning and susceptibility to biodegradation. The combustibility of wood can lead to severe economic losses, including threats to lives and livelihoods [1]. One of wood's critical material properties is its resistance to decay organisms, which usually determines its suitability for outdoor applications [2]. Various methods have been used to overcome such significant weaknesses in this material. The combustion behaviour of wood can be improved through the addition of fire retardants, with nitrogen-phophorous-based systems and halogenated compounds have been mostly used in timber application [3,4]. Similarly, its biodegradability can be improved through the use of biocides, which range from boron and copper compounds to azoles and creosote [5]. Due to their significant environmental impact, both are now under increasing scrutiny, making their use strictly controlled and limited, especially in ecologically sensitive environments [6]. The growing awareness has led to new opportunities for the development of alternative, environmentally friendly, non-hazardous, and halogen- and biocide-free wood modification methods. The use of natural materials has inspired many researchers to develop green wood modification strategies. One promising method to promote fire retardancy is the mineralization of wood [7]. Various minerals, such as silica [8], calcium oxalate [9], zinc borate [10], and struvite [11,12] have been incorporated into wood, with calcium carbonate receiving the most extensive study [13–16]. While the use of carbonates effectively reduces the burning intensity of wooden components, they often have a limited impact on extending the time to ignition. Recently, advancements have been made where

* Corresponding author.
** Corresponding author at: Slovenian National Building and Civil Engineering Institute, Dimičeva ulica 12, Ljubljana 1000, Slovenia.
E-mail addresses: andreja.pondelak@zag.si (A. Pondelak), andrijana.skapin@zag.si (A.S. Škapin).

https://doi.org/10.1016/j.conbuildmat.2026.146355
Received 20 November 2025; Received in revised form 11 April 2026; Accepted 13 April 2026
Available online 17 April 2026

magnesium ions were employed to promote the mineralization of $CaCO_3$ within wood, resulting in the formation of Mg-$CaCO_3$ and Mg calcite [17]. Due to the lower decomposition temperatures of magnesium carbonates [18] compared to calcium carbonate [19], thermal analysis suggests that using the former as fire retardant is more effective due to their lower decomposition temperatures. Fig. 1 illustrates the advantages of hydromagnesite, one of the representatives of magnesium carbonates, for wood mineralization compared to vaterite, a crystal form of calcium carbonate. The SEM images (Fig. 1a,b), the temperatures of the physicochemical changes (Fig. 1c,d) and the types of by-products released (Fig. 1e,f) during the decomposition of both minerals produced *via* calcium and magnesium acetoacetate, respectively, are

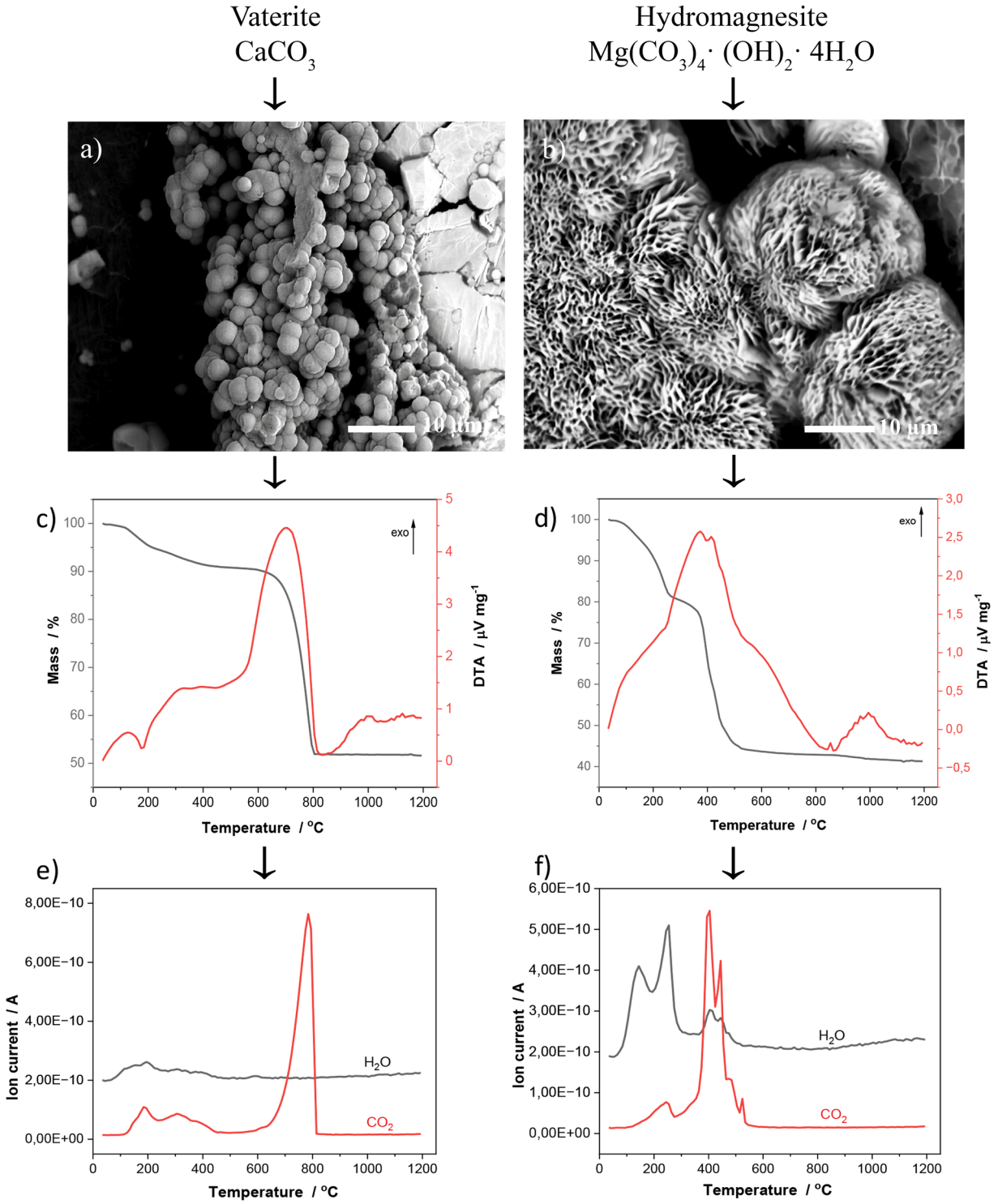

Fig. 1. Original experimental data highlighting the key properties of $CaCO_3$, vaterite (left column) and $Mg_5(CO_3)_4(OH)_2{\cdot}4\ H_2O$, hydromagnesite, (right column) highlighting the advantages of hydromagnesite for wood mineralization. (a,b) SEM images of vaterite and hydromagnesite formed during the decomposition of Ca $(OAcAc)_2$ and $Mg(OAcAc)_2$ solutions, used as traditional and novel impregnation reagents, respectively, in the wood mineralization process. (c,d) TG/DTA (black/red curves) profiles of vaterite and hydromagnesite, respectively. (e,f) MS curves - the ion currents of CO_2 ($m/z = 44$), and H_2O ($m/z = 18$) released from the vaterite and hydromagnesite, respectively.

presented. The TG/DTA profiles (Fig. 1c,d) and the ion currents of CO_2 and H_2O released (Fig. 1e,f) during the thermal decomposition of vaterite and hydromagnesite show that hydromagnesite decomposes endothermically at a lower temperature and releases H_2O besides CO_2, which is beneficial for fire protection. Unlike calcium carbonate, which remains stable until temperatures exceed 600 °C, magnesium carbonate hydrates undergo multi-stage endothermic decomposition that initiates < 250 °C which aligns precisely with the temperature range of wood pyrolysis. Rothon [20] has identified several magnesium carbonates—specifically nesquehonite, hydromagnesite, and magnesium carbonate subhydrate—as promising flame retardants for use in polymer composites. Each of these minerals decomposes endothermically, releasing carbon dioxide, water, or both. Among them, hydromagnesite has attracted the most commercial interest [21]. The thermal decomposition of hydromagnesite, $Mg_5(CO_3)_4(OH)_2{\cdot}4\,H_2O$, has been shown [22] to proceed through three distinct stages: dehydration, involving the removal of water of crystallization (<250 °C); dehydroxylation, where $Mg(OH)_2$ decomposes to MgO (about 250–350 °C); and decarbonation, during which $MgCO_3$ breaks down to MgO (occurring at higher temperatures >350 °C). This process has been described in more detail elsewhere [22–25], where it was shown, among others, that the decomposition mechanism depends on the heating rate and on the surrounding gaseous atmospheres at varying partial pressures.

To date, several studies in the literature demonstrate that magnesium carbonates enhance fire resistance in polymers [20,21,26], yet only a few have investigated their use as flame retardants in different wood-based composites [27–29]. Wu et al. [27] demonstrated that all three studied magnesium compounds—hydromagnesite, magnesium hydroxide, and magnesium chloride hexahydrate—offered effective protection against fire for wood composites made from red gum wood powder. Yılmaz Atay [28] developed the flame-retardant wood composites using sawdust combined with huntite and hydromagnesite minerals. Ustaömer and Başer [29] investigated the fire performance of fiberboards produced with huntite/hydromagnesite and zinc borate. The same research group reported [30] that huntite/hydromagnesite and zinc borate positively affected the biological properties of fiberboard samples, suggesting their potential for protecting wood against biological deterioration. While these traditional magnesium-based treatments are effective for wood-based composites, they are often unsuitable for solid wood due to limited penetration depth and the formation of corrosive by-products. Even in these limited cases, the focus has been on incorporating these minerals into wood composites rather than solid wood, primarily because the greatest challenge with solid wood is achieving deep mineral penetration, ensuring that reagents are evenly distributed across its cross-section, since the minerals tend to remain near the surface during impregnation. Our recent research successfully overcame this challenge, but the focus was on the less effective calcium carbonate [15]. The solid wood has been successfully mineralized and exhibited improvements in both flame retardancy [15] and fungal durability [16] compared to native wood.

In this article, by taking into account all findings regarding magnesium carbonates as the promising fire retardants and overcoming obstacles of impregnation solid wood deep in its structure we demonstrate the halogen- and biocide-free in-situ formation of magnesium carbonates deep in the structure of solid wood, using vacuum-pressure impregnation with a single-component treatment agent – namely, a water solution of magnesium acetoacetate, $Mg(OOCCH_2COCH_3)_2$, hereinafter abbreviated to $Mg(OAcAc)_2$. The major objective of this study is to demonstrate that novel halogen- and biocide-free solid mineral-wood composites effectively enhances fire resistance, due to its favourable endothermic decomposition of magnesium carbonates at lower temperatures, while also providing excellent protection against fungi through increased alkalinity (pH 9.4), thus promoting the substitution of hazardous and environmentally detrimental wood treatment options. To our knowledge, this is the first study to explore the use of magnesium carbonates in solid wood mineralization and its impact on both fire and fungal resistance, whereas previous research has been limited to wood composites [27–30]. Unlike calcium-based systems the $Mg(OAcAc)_2$ forms diverse hydrated and basic phases that provide a unique synergistic protection mechanism. Specifically, these phases decompose at temperatures that precisely match wood pyrolysis, a functionality that anhydrous $CaCO_3$ lacks.

2. Materials and methods

2.1. Materials and chemicals

European beech wood (*Fagus sylvatica*) and Norway spruce wood (*Picea abies*), free from visible defects and harvested from a forest in Slovenia, were used throughout the study. Wood boards measuring 520 mm × 100 mm × 10 mm were initially prepared for the mineralization process. Following the treatment, these boards were cut into 100 mm× 100 mm× 10 mm specimens specifically for cone calorimetry. For fungal durability tests, samples were initially prepared in dimensions of 50 mm × 25 mm × 15 mm according to EN 113–1. Specimens for TGA/DTA, FE-SEM, XRD, EMC, and pH measurements were further sub-sampled from the 50 mm × 25 mm × 15 mm blocks to meet analytical requirements. For examination of the penetration depth by XRF, samples measuring 50 mm × 25 mm × 15 mm were impregnated. Prior to the mineralization process, all specimens were conditioned at 20 °C and 65% RH until they reached a constant mass, resulting in an initial moisture content of approximately 11.8%. The average oven-dry density was 422 kg/m^3 for spruce wood and 685 kg/m^3 for beech wood.

2.2. Wood mineralization

The mineralization of wood was performed *via* vacuum-pressure impregnation using a 20 wt% water solution of magnesium acetoacetate, $Mg(OAcAc)_2$, (corresponding to the theoretical formation of 7.4 wt % $MgCO_3$). $Mg(OAcAc)_2$ was selected as a precursor due to its high-water solubility, which ensures deep penetration into the solid wood structure, and its thermal instability, which allows controlled in-situ transformation into various insoluble magnesium carbonates. Preliminary tests indicated that a 10 wt% solution provided insufficient mineral loading, while concentrations exceeding 20 wt% (e.g., 30 wt%) resulted in increased solution viscosity. This approach enables mineralization of wood without the formation of solid by-products that could block pore accessibility.

The wood specimens were fully submerged in the $Mg(OAcAc)_2$ solution within a vessel before being placed in the chamber. Both the precursor synthesis and the subsequent mineralization treatment were conducted in accordance with the patented process [31]. To ensure the stability of the precursor, the $Mg(OAcAc)_2$ solution was stored at sub-zero temperatures and brought to room temperature only immediately before the impregnation process. The impregnation process consisted of four steps. In the first step, the submerged wood specimens were exposed to a vacuum at 50–60 mbar for 30 min, before reducing the pressure back to normal. In the second stage, the wood specimens were exposed to a pressure of 8–10 bars for 3 h, then the pressure was reduced back to normal. The third stage repeated the first stage, exposure to a vacuum of 50–60 mbar for 30 min. The third stage was applied to remove excess impregnation solution from the wood surfaces and macro-pores. This prevents exudation and results in a clean surface without the need for additional washing, as confirmed by visual inspection which showed no white mineral residues on the surface of the samples. In the final, fourth stage, known as the post-treatment stage, the impregnated wood specimens were firstly dried for 3 days at room temperature and then placed into a chamber with elevated temperature and relative humidity (80 °C and 100% RH, respectively) for a further 3 days. The elevated temperature and humidity in the final stage are critical to accelerate the in-situ transformation of the soluble Mg

$(OAcAc)_2$ precursor into insoluble magnesium carbonate-based minerals through hydrolysis and thermal decomposition. The mineralized wood was then stored for 14 days under standard laboratory conditions (23 °C and 50% RH) before testing. The use of this post-treatment process allows the impregnating agent ($Mg(OAcAc)_2$) to be converted into magnesium carbonate-based compounds. The selection of a 20 wt% Mg $(OAcAc)_2$ concentration and the post-treatment parameters (80 °C / 100% RH) was based on established protocols from prior wood mineralization research using calcium acetoacetate precursors [31]. Although these parameters effectively achieved the study's objectives, further systematic optimization of precursor concentration and post-treatment conditions could be explored in future work to maximize mineral yield and performance.

2.3. Measurements and characterization

A thermal decomposition of carbonates was studied by thermogravimetric analysis (TGA) and differential thermal analysis (DTA) on a Netzsch Jupiter 449 simultaneous thermal analysis instrument coupled with a mass spectrometer (MS) (Netzsch QMS 403 C Aeolos quadrupole). The analysis was performed in synthetic air from 40 °C to 1200 °C with a heating rate of 10 °C/min using an alumina crucible with a lid. The evolution of H_2O and CO_2 was monitored by *m/z* fragments of 18, and *m/z* fragments of 44, respectively.

The crystalline phases of the precipitated samples as well as the impregnated woods were analyzed by X-ray powder diffraction (XRD) using a D4 Endeavor Bruker AXS diffractometer, measured at 2 Q range from 10 to 70°, a step size of 0.04° and a collection time of 3 s using $CuKa_1$ radiation.

Micro-XRF mapping (Bruker M4 Tornado μ-XRF spectrometer, with a rhodium (Rh) X-ray source) was performed on a cross-section of mineralised beech and spruce wood samples. Elemental maps were collected at 50 kV and 300 μA with a vacuum (20 mbar = 2000 Pa). The analyses were conducted with a spot size of 20 μm and a spot distance of 150 μm. One cycle was done for each map, with a dwell time of 15 mm/s for each measure. Data processing was carried out using the Bruker M4 Tornado software.

The morphology, shape and distribution of magnesium carbonate-based particles formed within the structure of the wood were investigated using FE-SEM (Zeiss ULTRA plus). FE-SEM images were performed in high vacuum with an InLens detector, using an electron acceleration of 3–5 kV and a working distance of 2–5 mm. The samples were cut by a cross-section polisher (JEOL SM-09010, Japan), placed on double-sided carbon tape and additionally Pt-coated prior to examination using a Gatan 682 Precision and Etching System (PECS). The thickness of the Pt coating was 3 nm. The distribution, shape and size of magnesium carbonate-based particles incorporated inside the wood were examined by an Xradia μCT-400 tomograph (XRadia, Concord, California, USA), with the images obtained using a 20X magnification optical objective, a working voltage of 40 kV, 125 μA energy and a spatial resolution of 0.88 μm. The size of the specimens was approximately 40 mm in length and 2 mm in diameter.

The reaction to fire parameters of the native and mineralized wood were measured using cone calorimetric tests (Fire Testing Technologies, UK), following the procedure outlined in ISO 5660–1 and using an incident heat flux of 50 kW/m^2. The size of the specimens was 100 mm× 100 mm x 10 mm. The cone data presented are the average values of five parallel measurements. The reaction to fire characteristics were simulated using ConeTools software.

The equilibrium moisture content (EMC) of the native and mineralized wood was determined according to EN 13183–1:2002. The native and mineralized wood specimens were oven-dried at 103 °C ± 2 °C to a constant mass (absolute dry) then stored in a climatic chamber (23 °C and 65% RH) until a constant mass (equilibrium moisture content) was achieved. The EMC values presented are the average of five parallel measurements.

The pH values of the native and mineralized wood surfaces were measured on laboratory-conditioned specimens (23 °C and 50% RH) using a Titrino probe with a flat electrode. Firstly, 3 mL of deionised water was placed on the wood's surface, then the probe was placed in contact with the surface. Once stable, the pH value was recorded. All measurements were performed in a room subject to laboratory conditions (T = 20 °C, RH = 65%), with the average of five parallel measurements recorded.

Fungal durability was performed according to the European standard EN 113–1 (2021). Two different fungi were used: brown rot fungi, *Gloeophyllum trabeum,* and white rot fungi, *Trametes versicolor*. The fungi originated from the fungal collection of the Biotechnical Faculty, University of Ljubljana, which is available to research institutions upon request. Five replicates were prepared for each type of material and fungi. The resulting mass loss (Δm) is calculated as the difference between the absolute mass of specimens prior to fungal exposure (m_0) and the absolute mass of specimens after fungal exposure (m_1), divided by m_0 and multiplied by 100. Full details of the method used are provided elsewhere [32].

To assess the statistical significance of differences between native and mineralized wood, an independent samples *t*-test was performed for relevant measured parameters (cone calorimetry, EMC, pH, and fungal mass loss). The results were categorized into levels of significance: $p < 0.05$ (*), $p < 0.01$ (**), and $p < 0.001$ (***). Differences with $p \geq 0.05$ were considered not significant (ns).

3. Results and discussion

3.1. The process of wood mineralization

The two most common wood species in Europe, European beech (*Fagus sylvatica*) and Norway spruce (*Picea abies*), were selected for investigation in this study. The wood was impregnated with a water solution of magnesium acetoacetate ($Mg(OAcAc)_2$) as a precursor for the synthesis of $MgCO_3$-based compounds. Fig. 2 demonstrates the process of $MgCO_3$-based wood mineralization using this method. Firstly, a vessel containing the wood samples is filled with the impregnation solution and placed in a vacuum–pressure chamber. Using a vacuum-pressure full cell process the impregnation solution then penetrates through cross sections of the wood specimens. In the final (post-treatment) step, the $Mg(OAcAc)_2$ impregnation solution transforms into $MgCO_3$-based compounds.

Namely, in the presence of water or moisture in the air, the acetoacetate ion decomposes into a carbonate and/or hydroxide and/or oxide ion, carbon dioxide and acetone. The latter two evaporate, leaving a solid carbonate, hydroxide or oxide. The reaction (1) demonstrates the conversion of the acetoacetate ion into a carbonate ion:

$$2CH_3COCH_2COO^- + H_2O \rightarrow CO_3^{2-} + CO_2 + 2CH_3COCH_3 \quad (1)$$

Following the generation of carbonate ions (reaction 1), these ions rapidly react with the liberated cations and available moisture to precipitate various magnesium carbonate-based minerals. Different magnesium carbonate-based compounds can be formed, including nesquehonite [$MgCO_3 \cdot 3\,H_2O$], hydromagnesite [$Mg_5(CO_3)_4 \cdot (OH)_2 \cdot 4\,H_2O$], oxymagnesite [$MgO \cdot 2MgCO_3$], giorgiosite [$Mg_5(CO_3)_4 \cdot (OH)_2 \cdot 5–6H_2O$] and anhydrous magnesite [$MgCO_3$] [33,34]. Our experimental observations showed that nesquehonite formed predominantly in mineralized Norway spruce, while giorgiosite was the primary

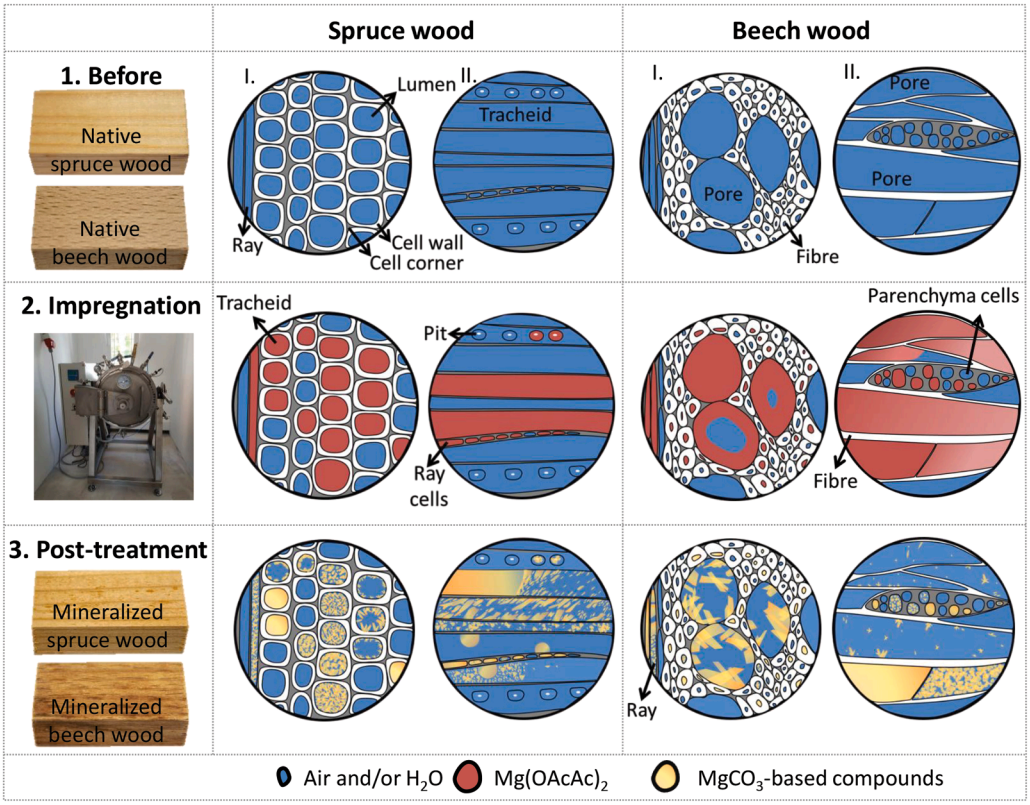

Fig. 2. Photographs of wood specimens and schematic morphological structure of the spruce and beech wood (1) before, (2) after impregnation, and (3) after post-treatment. The schematics represent the process of $Mg(OAcAc)_2$ mineralization in spruce wood middle column) and beech wood (right column), shown in (I) cross-section and (II) tangential section. In each column, the illustrations represent a magnified structure of the wood – from top to bottom: before mineralization, after impregnation, and following precipitation of the $MgCO_3$-based compounds.

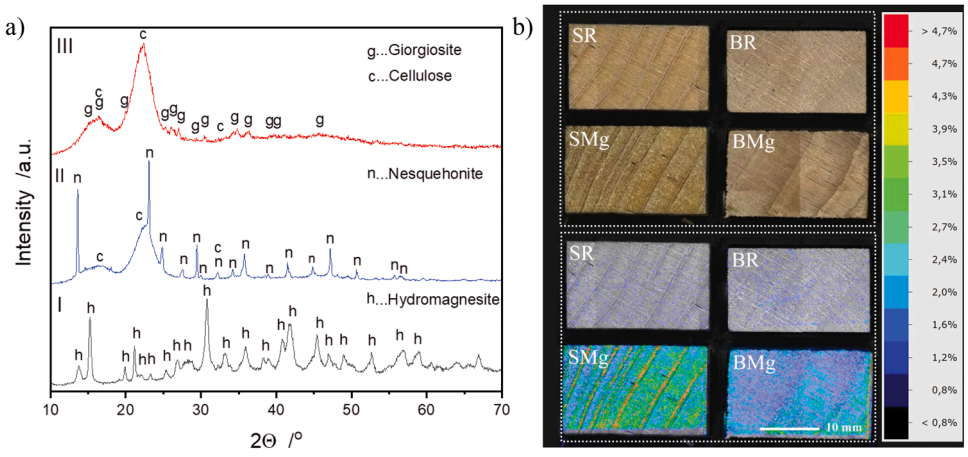

Fig. 3. (a) XRD patterns of: (I) hydromagnesite (ICDD No. 00–025-0513), (II) spruce wood treated by $Mg(OAcAc)_2$ - cellulose (ICDD No. 00–030-0223) and nesquehonite (ICDD No. 00–020-0669) and (III) beech wood treated by $Mg(OAcAc)_2$ - cellulose (ICDD No. 00–030-0223) and giorgiosite (ICDD No. 00–029-0858); (b) Photographs and corresponding micro-XRF mapps of the cross-sections for native and mineralized spruce and beech wood samples: The top rows show photographs of the native (SR, BR) and mineralized (SMg, BMg) samples, while the bottom rows display the Micro-XRF elemental mapping of magnesium (Mg). The color scale indicates the Mg concentration (wt%). Legend: SR – native spruce wood; SMg – mineralized spruce wood; BR – native beech wood; BMg – mineralized beech wood, c – cellulose, g – giorgiosite, n – nesquehonite, h - hydromagnesite.

phase identified in mineralized European beech within the investigated system, as confirmed by XRD analysis (Fig. 3a). XRD pattern of mineralized spruce wood (II) shows reflections of cellulose and nesquehonite, while XRD pattern of treated beech wood (III) shows reflections corresponding to cellulose and giorgiosite. In contrast, hydromagnesite (highlighted in Fig. 1) was the dominant phase when the $Mg(OAcAc)_2$ precursor, subjected to the same experimental protocol as the wood samples, was decomposed in a wood-free environment (petri dish), as also confirmed by XRD. All reflections (XRD pattern (I) in Fig. 3a) belong to hydromagnesite. The formation of hydromagnesite, nesquehonite and giorgiosite can be described by Reactions (2), (3) and (4), respectively:

$$5\,Mg(CH_3COCH_2COO)_2 + 10\,H_2O \rightarrow Mg_5(CO_3)_4(OH)_2{\cdot}4\,H_2O + 6\,CO_2 + 10\,CH_3COCH_3 \quad (2)$$

$$Mg(CH_3COCH_2COO)_2 + 4\,H_2O \rightarrow Mg(CO_3){\cdot}3\,H_2O + CO_2 + 2\,CH_3COCH_3 \quad (3)$$

$$5\,Mg(CH_3COCH_2COO)_2 + 11 - 12\,H_2O \rightarrow Mg_5(CO_3)_4(OH)_2{\cdot}5 - 6\,H_2O + 6\,CO_2 + 10\,CH_3COCH_3 \quad (4)$$

The term 'MgCO$_3$-based compounds' is used throughout the rest of this paper to refer to this type of compounds. A single impregnation trial using a 20 wt% aqueous Mg(OAcAc)$_2$ solution resulted in the formation of (10.0 ± 3.6) wt% and (6.1 ± 0.4) wt% MgCO$_3$-based compounds in spruce and beech wood, respectively (Table 1).

Visual inspection of the specimens before and after treatment (Fig. 2, far left column, and Fig. 3b, upper four photographs) confirms that the mineralization process does not significantly alter the natural colour or aesthetic appearance of Norway spruce and European beech. In order to evaluate the penetration depth and spatial distribution of the MgCO$_3$-based minerals, mineralized wood specimens with dimensions of 50 mm × 25 mm × 15 mm were analyzed. After the mineralization treatment, the samples were cut in half and the distribution of Mg across internal cross-sections was determined using Micro-XRF elemental mapping (Fig. 3b). In both mineralized spruce wood (SMg) and beech wood (BMg) samples, the Mg signal is clearly detected across the full cross-sectional area, confirming the successful incorporation of magnesium throughout the samples.

4. Incorporation of the minerals into the structure of the wood

The distribution, shape and size of the resulting particles inside the wood were investigated by microcomputed tomography (μCT) and scanning electron microscopy (SEM). The schematic representation in Fig. 2 provides an idealized visualization of the mineralization stages, derived from the synthesis of extensive SEM and μCT imaging data to illustrate the distribution of minerals within the wood's microscopic features. As illustrated (Fig. 2), under vacuum–pressure the impregnated Mg(OAcAc)$_2$ aqueous solution fills different anatomical structures of the wood (i.e. tracheids, ray cells and pits), where it is later transformed into MgCO$_3$-based particles. The microstructures of different sections of the mineralized wood, as investigated by μCT and SEM, are shown in Figs. 4 and 5 for spruce wood and beech wood, respectively. In spruce wood, the fluid intake of the impregnating solutions causes MgCO$_3$-based particles to be distributed along the tracheid (as evident in Fig. 4b,c,g), in rays (Fig. 4d) and on and inside the pits (Fig. 4i). The particles formed are mainly needles (Fig. 4d,e,g,h,i), or irregular particles, as seen in Fig. 4f, which shows the lumina filling.

The incorporation of MgCO$_3$-based particles into beech wood is presented in Fig. 5. Based on the presence of MgCO$_3$-based compounds, as confirmed by μCT and SEM investigation (Fig. 5), it can be concluded that the fluid intake of the impregnating solutions is mostly integrated in all the main anatomical structures of the wood i.e. in pores, fibers and parenchyma cells. The particles are mainly in needle (Fig. 5d,e,g) or irregular form (Fig. 5f,h,i), like as in the mineralized spruce wood. The needle-like shapes defined are found in pores, while the irregular ones are found in fibers and parenchyma cells.

The pore volume and pore size distribution of the selected wood species dictates the sorption behaviour of impregnation solutions [35] and, consequently, the shape and size of the MgCO$_3$-based particles formed. The pore diameters of tracheids are much smaller in softwood than they are in hardwood; the diameter of tracheids in softwoods are typically between 10 μm and 50 μm, while in hardwood pore diameters can range from 50 μm to 400 μm in spring wood, and from 20 μm to 50 μm in autumn wood [35]. Particles formed in the tracheids of the spruce wood (Fig. 4d,e) were smaller than those formed in the pores of beech wood (Fig. 5d,e,g,h). Wood is a highly inhomogeneous material, with anatomical variability between earlywood and latewood, heartwood and sapwood, and across cell types, which can strongly influence fluid penetration and local mineral uptake. During sample preparation, especially cutting, polishing, or washing, part of the minerals deposited in cell lumina or weakly bound to cell walls may be partially removed, further contributing to the apparent uneven distribution in the image. Moreover, based on the observed mass increase, it is not expected that the wood would be fully or uniformly impregnated with Mg(OAcAc)$_2$ solution, and differences in treatment cycles (pressure–vacuum efficiency, diffusion time, moisture content) could additionally contribute

Table 1
Mass of MgCO$_3$-based compounds formed, cone calorimetry data, equilibrium moisture content (EMC) and pH values for spruce and beech wood both before and after mineralization. The column on the far-right shows data for beech wood mineralized with CaCO$_3$ for comparison. [$t_{ignition}$ – time of ignition; $THR_{600\,s}$ – total heat release in the first 600 s of the test; FIGRA – fire growth rate index; TSP – total smoke production; PHRR – peaks of heat release rate].

		Native spruce wood	Spruce wood mineralized by MgCO$_3$-based compounds	*Average difference after min. [%]*	Native beech wood	Beech wood mineralized by MgCO$_3$-based compounds	*Average difference after min. [%]*	Beech wood mineralized by CaCO$_3$
Weight gain - m_{MgCO3}[a]	(%)	/	10.0 ± 3.6	/	/	6.1 ± 0.4	/	7.4 ± 1.3[14] 12 ± 4[15, 22]
$t_{ignition}$[b]	(s)	20.8 ± 2.6	31.8 ± 4.5 **	*+ 53*	29.8 ± 3.8	46.2 ± 3.8 ***	*+ 55*	46.8 ± 6.2[14]
$THR_{600\,s}$[b]	(MJ)	21.0 ± 0.4	19.1 ± 1.5 *	*-9*	43.5 ± 2.7	31.3 ± 1.9 ***	*-28*	31.8 ± 2.1[14]
FIGRA[b]	(Ws^{-1})	372.6 ± 50.3	223.0 ± 35.7 ***	*-40*	530.3 ± 51.0	203.9 ± 20.7 ***	*-62*	217.2 ± 9.4[14]
TSP[b]	(m^2)	2.0 ± 0.5	0.8 ± 0.1 **	*-60*	2.5 ± 1.0	1.4 ± 0.2 'ns'	*-44*	/
$t_{1.\,pHRR}$[b]	(s)	23 ± 4.5	33 ± 4.5 **	*+ 43*	36.4 ± 5.9	52 ± 3.0 ***	*+ 43*	52 ± 7.6[14]
1. $_{pHRR}$[b]	(kWm^{-2})	185.3 ± 25.6	177.2 ± 12.5 'ns'	*-5*	219.2 ± 9.1	175 ± 8.6 ***	*-20*	179 ± 11.6[14]
$t_{2.\,pHRR}$[b]	(s)	354.2 ± 11.4	381.1 ± 26.4 'ns'	*+ 8*	277.0 ± 19.6	436 ± 16.5 ***	*+ 57*	392 ± 4.5[14]
2. $_{pHRR}$[b]	(kWm^{-2})	180.2 ± 11.8	185.8 ± 23.5 'ns'	*+ 3*	509.6 ± 53.4	335.0 ± 40.4 ***	*-34*	375 ± 33.0[14]
EMC $_{65\%}$	(%)	10.6 ± 0.1	10.3 ± 0.1 ***	*-3*	10.2 ± 0.1	11.2 ± 0.2 ***	*+ 10*	10.1 ± 0.2[15]
pH value	(/)	5.5 ± 0.3	9.4 ± 0.1 ***	*+ 71*	5.4 ± 0.5	9.4 ± 0.3 ***	*+ 74*	8.07 ± 0.3[15]

Notes: Asterisks indicate the level of statistical significance compared to the native sample: * $p < 0.05$ (significant), ** $p < 0.01$ (highly significant), and *** $p < 0.001$ (very highly significant), as determined by an independent samples *t*-test. 'ns' indicates a non-significant difference ($p \geq 0.05$).

[a] Determined by the difference in mass between oven-dry samples before and after mineralization (mass of MgCO$_3$ per mass of sample);

[b] Determined from cone calorimetry, through exposure to a constant irradiation of 50 kW m^{-2};

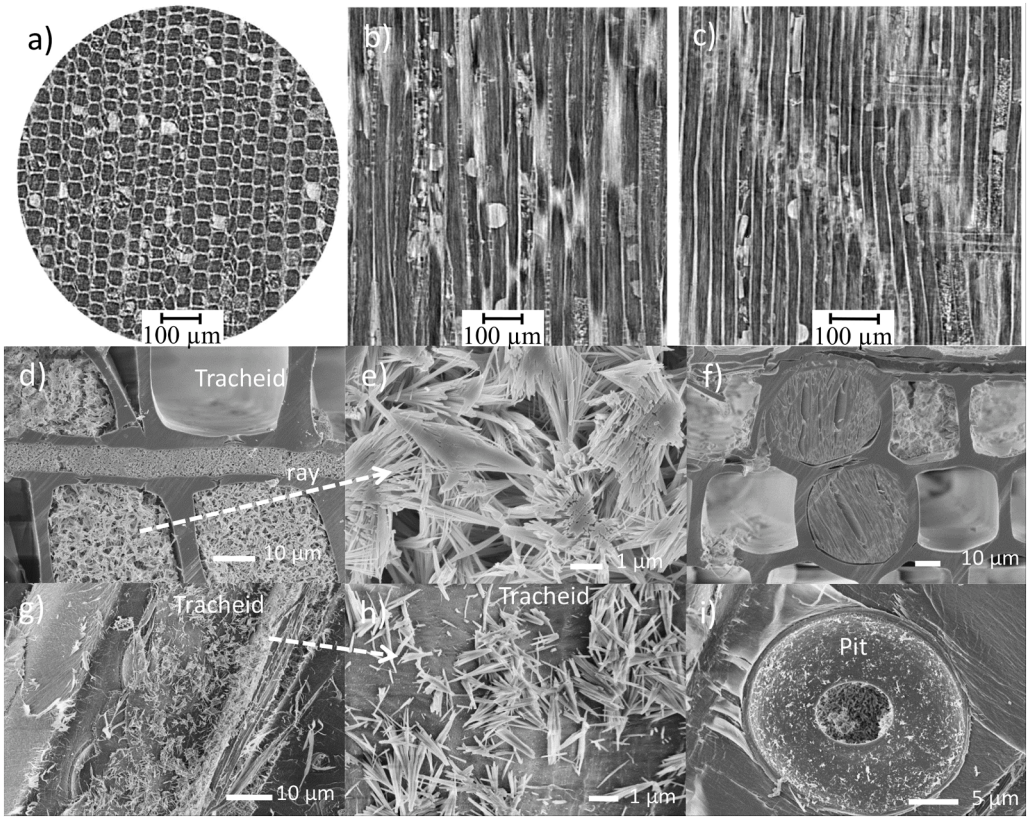

Fig. 4. Structural characterization of spruce wood mineralized with $MgCO_3$-based compounds. µCT images of the (a) transverse, (b) tangential and (c) radial sections and SEM micrographs of the (d–f) cross sections and (g–i) tangential sections of mineralized spruce wood.

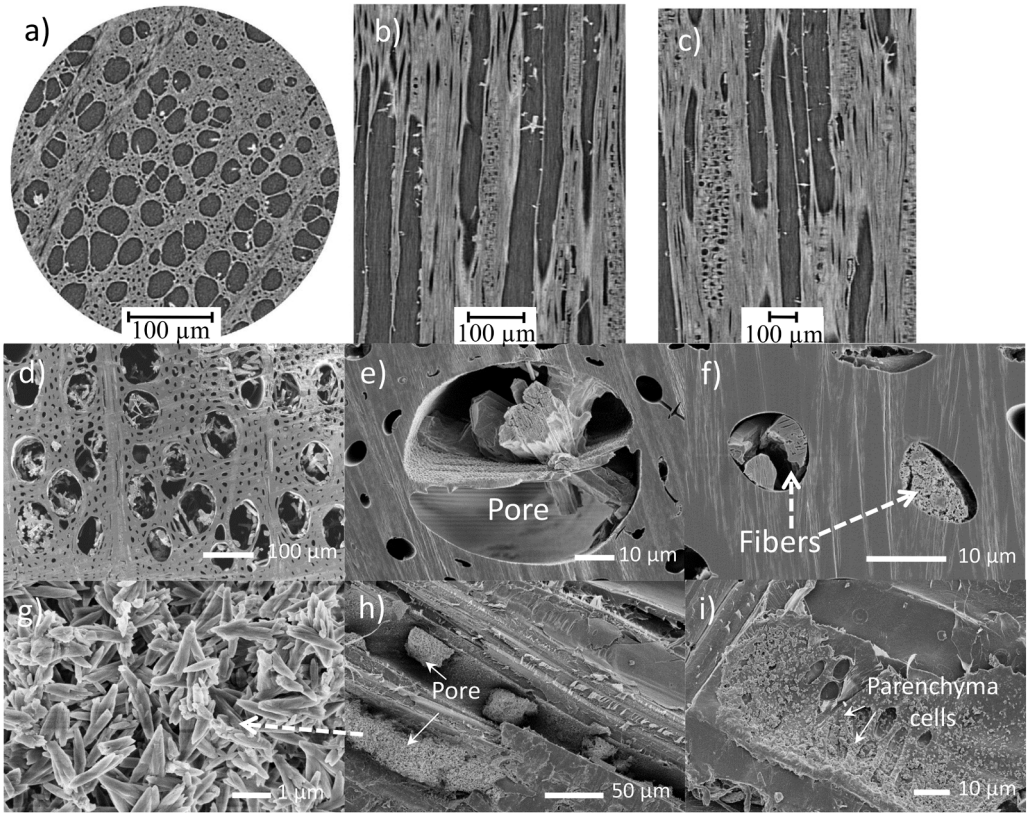

Fig. 5. Structural characterization of beech wood mineralized with $MgCO_3$-based compounds. µCT images of the (a) transverse, (b) tangential and (c) radial sections and SEM micrographs of the (d–f) cross sections and (g–i) tangential sections of mineralized beech wood.

to localized variations in mineral content.

The successful deposition of $MgCO_3$-based particles within the voids (tracheids, rays, and pores) suggests a reinforcing pore-filling effect rather than structural degradation. This microstructural evidence showing no chemical changes to the wood fibers, indicates that the mineralization process preserves the integrity of the wood substrate.

5. Fire performance

The effect of novel mineralization on the reaction of wood to fire was determined using a cone calorimeter. Table 1 summarizes data regarding the fire parameters of native spruce and beech wood, and those for each species mineralized with $MgCO_3$-based compounds. The data for beech wood mineralized with $CaCO_3$, as previously published elsewhere [15,16,32], are presented in the column on the far right. In both spruce and beech wood, the fire characteristics measured - namely, the ignition time ($t_{ignition}$), total heat release in the first 600 s of the test ($THR_{600\ s}$), fire growth rate index (FIGRA) and total smoke production (TSP) - are significantly improved in the samples mineralized with $MgCO_3$-based compounds compared to the native samples (Table 1). Following mineralization, the time to ignition was prolonged by 53% in the spruce and 55% in the beech samples, whilst the $THR_{600\ s}$ values reduced by 9% and 28% and the FIGRA values by 40% and 62% in spruce and beech wood, respectively. Each of these changes indicates an improvement in the wood's reaction to fire. Furthermore, TSP is significantly improved in the mineralized samples, with the total smoke production reduced by 60% in spruce and 44% in beech wood. Overall, the improvement in fire properties ($t_{ignition}$, $THR_{600\ s}$, FIGRA) observed was more significant in the mineralized beech than in the mineralized spruce wood, even though the relative mass uptake was lower in beech wood (10.0 ± 3.6% in spruce compared to 6.1 ± 0.4% in beech wood).

Heat release rate (HRR) is the most important parameter in the assessment of flammability. Fig. 6a.c shows the HRR profiles (heat release *vs* time) of the native wood (black dotted curve) and wood mineralized with $MgCO_3$-based compounds (full black curve), each based on the average of five measurements. The peaks of heat release rate (pHRR) on the HRR curves provides information about the burning behaviour of the material tested [36]. The first peak (t_1. pHRR, Table 1) occurs at the beginning of the test, when volatile pyrolysis gases are present in sufficient quantities to cause ignition. The heat generated by the combustion maintains pyrolysis, releasing more volatiles. This is followed by the formation of a thermally insulating layer of char. The char layer decreases heat flux from the flame to the pyrolysis front, thus slowing down the pyrolysis process. When the pyrolysis front reaches the underside of the material tested, the increased active surface involved in the burning process allows more volatiles to evaporate from the wood, and a second peak (t_2. pHRR) appears on the HRR curves. When no more volatiles are emitted, the flaming and smouldering combustion stops, leaving the wood glowing, and the HRR curve returns to steady state. As seen in Fig. 6a,c and Table 1, both the HRR peaks (t_1 and t_2) and the peak heat release rates (1^{st} and 2^{nd} $_{p}$HRR) of the mineralized wood are substantially smaller and occurred later. This indicates a lower fire growth rate and enhanced char stabilization.

The positive effect of the $MgCO_3$-based compounds as a flame

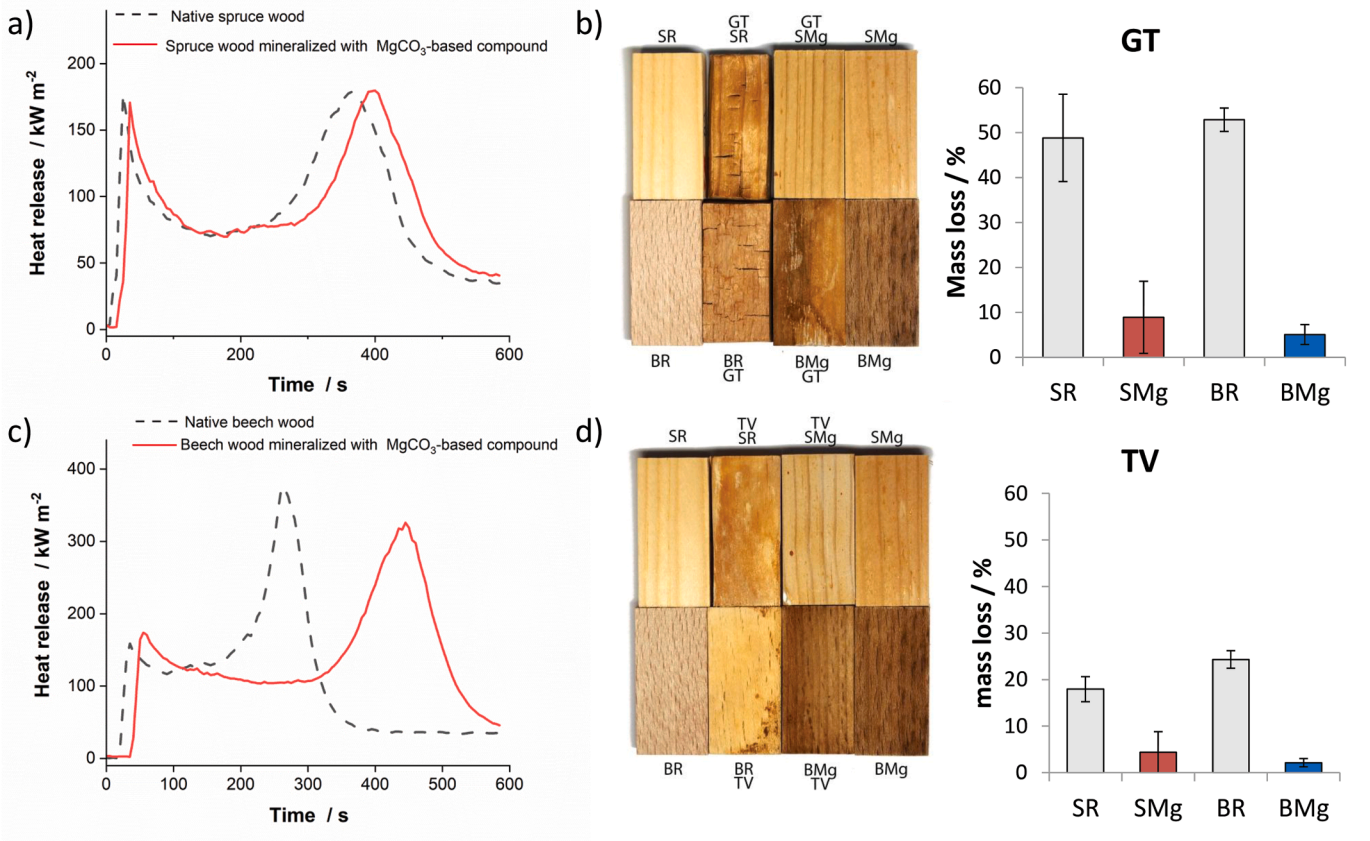

Fig. 6. Fire performance and fungal durability of the spruce and beech wood before and after mineralization. Heat release profiles of (a) the native (dotted curve) and $MgCO_3$-mineralized spruce (solid line) and (c) the native (dotted curve) and $MgCO_3$-mineralized beech wood (solid line). Photographs and mass loss (Δm) of the native and $MgCO_3$-based mineralized spruce and beech samples after 16 weeks of exposure to (b) *Gloeophyllum trabeum* (GT) and (d) *Trametes versicolor* (TV). In the bar charts (b and d), all mineralized specimens (SMg, BMg) exhibited very highly statistically significant reductions in mass loss compared to their respective native controls (SR, BR), as determined by an independent samples *t*-test ($p < 0.001$). In parts (b) and (d), the photographs show the native and mineralized samples before and after fungal exposure: unexposed native (far left), exposed native (second from left), unexposed mineralized (far right), and exposed mineralized (second from right) samples to GT (upper image) and TV fungi (lower image).

retardant during the combustion of wood is driven by an endothermic process, during which these compounds break down to MgO and release CO_2 and/ or H_2O (confirmed by TG-MS analysis - Fig. 1f), what cools and dilutes flammable gases in the event of a fire [13,15]. Moreover, the mineralization reduced the total smoke production (TSP) of the treated wood, by 60% in spruce and 44% in beech wood (Table 1).

Comparing the results to our previous study, which investigated the reaction to fire of $CaCO_3$ mineralized beech (far right column of Table 1) [15], it can be seen that mineralization with $MgCO_3$-based compounds improves the reaction to fire properties even further. While the type of carbonate used for the mineralization of beech wood has no influence on ignition time ($MgCO_3$ = 46.2 ± 3.8; $CaCO_3$ = 46.8 ± 6.2 [15]) or $THR_{600\,s}$ ($MgCO_3$ = 31.3 ± 1.9, $CaCO_3$ = 31.8 ± 2.1 [15]), the FIGRA values are better in the case of the $MgCO_3$-based compounds ($MgCO_3$ = 203.9 ± 20.7, $CaCO_3$= 217.2 ± 9.4 [15]). As previously mentioned, one of the reasons for this is the lower thermal decomposition temperature of $MgCO_3$ [18] compared to $CaCO_3$ [19]. Furthermore, in the case of using $MgCO_3$-based compounds, several types of hydrated and basic carbonates form, each with different ratios of carbonates and hydrates and varying numbers of bonded water molecules (i.e. nesquehonite [$MgCO_3$·3 H_2O], hydromagnesite [$Mg_5(CO_3)_4$·$(OH)_2$·4 H_2O], oxymagnesite [MgO·2$MgCO_3$], giorgiosite [$Mg_5(CO_3)_4$·$(OH)_2$·5–6H_2O] and anhydrous magnesite [$MgCO_3$] [33]). The various crystalline modifications of the $MgCO_3$-based compounds differ in terms of their crystal water content, which can additionally contribute to improvements in the fire performance of the wood. $CaCO_3$, on the other hand, is only found in its anhydrous form.

The more marked improvement in beech wood compared to spruce wood (Fig. 6c versus Fig. 6a), particularly the significant reduction in FIGRA and the second pHRR peak (Table 1), is due to its anatomical structure. Better permeability of beech wood facilitates the formation of substantial mineral deposits that act as a more effective physical barrier against heat and oxygen than the smaller deposits in spruce wood. Spruce wood is known as refractory species, what makes treatment of spruce wood more challenging. This can be the reason that the magnesium carbonate-based treatment is more effective at enhancing the char-forming capacity of hardwoods. Another reason for the more pronounced improvement in beech wood could be the different mineral phases formed in each wood species, with giorgiosite as the dominant phase in beech wood, as opposed to nesquehonite in spruce wood. The specific decomposition mechanisms of these phases may also contribute to the differences in efficiency regarding fire performance.

6. Fungal durability

The fungal durability of native wood and wood mineralized with $MgCO_3$-based compounds was determined by the mass loss (Δm) caused by brown (*Gloeophyllum trabeum)* and white (*Trametes versicolor*) rot fungi (Fig. 6b,d). Images of the unexposed native samples (far left) and the same samples after 16 weeks of fungal exposure (second from the left) are shown in Fig. 6b,d, alongside pictures of the mineralized samples before (far right) and after (second from the right) the fungal decomposition test.

The Δm in the mineralized spruce and beech wood is significantly lower than that in either of the native wood species (Fig. 6b,d), indicating that mineralization significantly improves resistance to the decay caused by the fungal species under investigation. At the end of the test, the mass loss in the mineralized spruce was, on average, 80% lower than that in the native spruce wood, while the Δm in the mineralized beech wood was about 90% lower than that observed in the non-treated wood. When samples were exposed to *Gloeophyllum trabeum,* Δm was higher than in the case of *Trametes versicolor*. In the case of the brown rot fungi [37], *Gloeophyllum trabeum,* the trend in Δm was similar for both species of wood. When exposed to the white rot fungus, *Trametes versicolor*, however, Δm was slightly higher in the beech wood, as expected, due to the fact that this fungus prefers hardwoods [37]. Based on the Δm recorded, the modified wood can be assigned durability classes according to CEN/TS 15083–1. As expected, the untreated wood can be classified into the lowest durability class, class 5 ('susceptible wood species'). Based on the Δm following exposure to the fungi, the modified beech wood can be classified into durability class 1 ('very durable'), while the modified spruce wood can be classified into durability class 2 ('durable'). It should be considered that only the most durable wood species (Cumaru, Azobe) and the best performing modified wood (Accoya, Kebony) is classified as very durable (durability class 1).

A key condition necessary for the fungal degradation of wood is the presence of moisture [37]. The equilibrium moisture content (EMC) for native spruce and native beech wood, determined under laboratory conditions (T = 20 °C; RH = 65%), is presented in Table 1, alongside the same data for each species mineralized with $MgCO_3$-based compounds. Generally, there is no significant difference between the EMC of the native wood and that of the mineralized wood, with the values ranging between 10.3% and 11.2%. Moreover, the temperature and pH can affect fungus growth and sporulation [38,39]. The pH values of the native and mineralized wood are also shown in Table 1. Following mineralization, both types of wood are alkaline (pH = 9.4), whereas the native wood species are slightly acidic (pH = 5.4–5.5). The data indicate that the most plausible reason for the improved fungal resistance of the mineralized wood is the increased pH value of the samples following mineralization. Most fungi grow better in acidic or neutral conditions (pH range of 3–7), with only a few species favouring neutral to slightly alkaline conditions [39]. Similar results were obtained in our previous study [36] investigating the fungal durability of $CaCO_3$-mineralized spruce and beech wood, which showed mineralized samples to be alkaline (pH values from 7.5 to 8.07 [16,32]). However, the authors acknowledge that pH plays an important role, but it is unlikely to be the sole mechanism responsible for the enhanced resistance of mineralised wood to wood-decay fungi. The mineral phase can contribute through alkalinity and pH buffering, helping maintain conditions less favourable for fungal growth and enzymatic activity, particularly when fungi attempt to acidify the substrate. At the same time, we propose that physical and transport-related effects are also significant. Specifically, the formation of luminal mineral crystals can partially occlude cell lumina and pit pathways, thereby reducing porosity and permeability. This occlusion may (i) restrict oxygen diffusion and lower oxygen availability within the wood, (ii) limit moisture and nutrient transport, and (iii) hinder hyphal penetration and spread through the cell network [40]. Collectively, these effects can slow microbiological colonisation and constrain the progression of decay, acting in parallel with any chemical effects associated with pH buffering. In addition, mineral deposition may reduce the availability of easily accessible carbohydrates by partially shielding cell wall surfaces from enzymatic attack, thereby decreasing the efficiency of fungal depolymerisation processes. The presence of inorganic phases within the lumina and at the cell wall interface can also modify the local microenvironment, potentially affect ion balance and interfere with the diffusion of low-molecular-weight metabolites that fungi use to initiate decay. Furthermore, mineral particles may increase the stiffness and dimensional stability of the wood matrix, thereby reducing microcracking and moisture redistribution, which in turn limits favourable niches for fungal establishment and sustained colonisation [41]. Overall, wood mineralized with $MgCO_3$--based compounds shows significantly greater resistance to fungi than wood mineralized with $CaCO_3$, treated using the same process and subjected to the same fungal test [36]. The Δm in $CaCO_3$-mineralized wood exposed to *Gloeophyllum trabeum* for 16 weeks, for example, was 36% in spruce and 20% in beech wood [36], compared to values of only 9% (spruce) and 5% (beech) in the wood mineralized with $MgCO_3$-based compounds. A similar trend was observed in the samples exposed to *Trametes versicolor*, where spruce and beech wood samples mineralized with $CaCO_3$ had a Δm of 12% and 18%, compared to respective values of only 4% and 2% in the case of mineralization with $MgCO_3$-based compounds. The better fungal resistance of wood mineralized with

$MgCO_3$-based compounds compared to $CaCO_3$-mineralized wood can be attributed to the even higher pH values of the former.

Compared to other magnesium-based materials, such as magnesium oxychloride cement (MOC) or $Mg(OH)_2$, presented method achieves deep in-situ mineralization of solid wood rather than acting as a binder for composites or a surface coating. The protective mechanism of the hydrated magnesium carbonate system coincides with the onset of wood pyrolysis, providing active cooling and gas dilution when it is most needed. This distinguishes presented approach from other magnesium treatments used on different substrates and wood species.

7. Conclusions

This study successfully demonstrate an innovative, environmentally friendly mineralization process using a water solution of magnesium acetoacetate ($Mg(OAcAc)_2$) that significantly improves the fire retardancy and enhances fungal resistance of solid Norway spruce wood (*Picea abies*) and European beech wood (*Fagus sylvatica*). The key findings are as follows:

- The vacuum-pressure treatment achieves deep penetration and in-situ formation of hydrated magnesium carbonate-based compounds throughout the solid wood structure.
- The treatment significantly improves wood's reaction to fire, prolonging the time to ignition by more than 50% - from an average of 20.8 s to 31.8 s in spruce and from 29.8 s to 46.2 s in the beech wood. Similarly, significant decreases were observed in the total heat release in the first 600 s of the test ($THR_{600\ s}$) and the fire growth rate index (FIGRA), whilst the total smoke production (TSP) was also lower in both wood species.
- The superior fire performance is attributed to the magnesium carbonates' thermal decomposition mechanism, which unlike anhydrous $CaCO_3$ decompose at lower temperatures, releasing both CO_2 and H_2O. This early onset aligns precisely with the temperature range of wood pyrolysis, providing effective cooling of the wood substrate and the dilution of flammable gases at critical ignition points.
- Resistance to decay is improved when mineralized spruce and beech wood exposed to brown (*Gloeophyllum trabeum)* and white (*Trametes versicolor*) rot fungi. The largest positive effect was found in the case of beech wood exposed to *Gloeophyllum trabeum,* where the mass loss decreased from 49% before mineralization to only 5% following application of the treatment process.
- The alkaline nature of the environment following the treatment (pH 9.4), compared to the more acidic environment (pH 5.4–5.5) of the native wood, is a key factor in inhibiting fungal growth. The results show that the transition to $MgCO_3$-based mineralization is a functional breakthrough rather than a simple cationic replacement. Achieving high alkalinity and aligning endothermic decomposition with the wood's thermal degradation range provide a dual-protection mechanism that significantly outperforms traditional treatments.

While these results are promising, the mineralization process reproducibility and the long-term leaching resistance of the mineralized compounds in exterior applications remain to be evaluated in future studies. This dual-function mineralization approach provides a viable, halogen- and biocide-free pathway for sustainable protection of solid timber in construction.

CRediT authorship contribution statement

Andreja Pondelak: Writing – review & editing, Writing – original draft, Visualization, Investigation, Data curation, Conceptualization. **Nataša Knez:** Writing – review & editing, Investigation. **Srečo Davor Škapin:** Writing – review & editing, Investigation. **Miha Humar:** Writing – review & editing, Validation. **Andrijana Sever Škapin:** Writing – review & editing, Validation, Funding acquisition.

Declaration of Competing Interest

The authors declare the following financial interests/personal relationships which may be considered as potential competing interests: Andreja Pondelak has patent #EP 3 934 869 B1 issued to assignee. If there are other authors, they declare that they have no known competing financial interests or personal relationships that could have appeared to influence the work reported in this paper.

Acknowledgements

We are very much obliged to Mrs. Catherine Earles for proof-reading the English manuscript. This work was supported by the Slovenian Research and Innovation Agency (Grant numbers J7–50231, J1–3026, P4–0430, P2–0273 and P4–0015).

Data availability

The data presented in this study will be openly available from the repository DiRROS: http://hdl.handle.net/20.500.12556/DiRROS-22306 and upon request from the first and corresponding author.

References

[1] R.A. Mensah, L. Jiang, J.S. Renner, Q. Xu, Characterisation of the fire behaviour of wood: from pyrolysis to fire retardant mechanisms, J. Therm. Anal. Calor. 148 (2023) 1407–1422, https://doi.org/10.1007/s10973-022-11442-0.
[2] C. Brischke, G. Alfredsen, L. Emmerich, M. Humar, L. Meyer-Veltrup, Durability of wood exposed above ground-experience with the bundle test method, Forests 14 (2023), https://doi.org/10.3390/f14071460.
[3] A.B. Morgan, J.W. Gilman, An overview of flame retardancy of polymeric materials: application, technology, and future directions, Fire Mater. 37 (2013) 259–279, https://doi.org/10.1002/fam.2128.
[4] S. Dan, R. Kumar, Development of nitrogen-phosphorous and nano-SiO2-based fire retardant system for improved thermal, mechanical, and flame retardant properties in wood, Constr. Build. Mater. 485 (2025) 141786, https://doi.org/10.1016/j.conbuildmat.2025.141786.
[5] B. Goodell, J.E. Winandy, J.J. Morrell, Fungal degradation of wood: emerging data, new insights and changing perceptions, Coatings 10 (2020), https://doi.org/10.3390/coatings10121210.
[6] P. Gerardin, New alternatives for wood preservation based on thermal and chemical modification of wood- a review, Ann. For. Sci. 73 (2016) 559–570, https://doi.org/10.1007/s13595-015-0531-4.
[7] R.F. Beims, R. Arredondo, D.J.S. Carrero, Z.S. Yuan, H.W. Li, H.F. Shui, Y.S. Zhang, M. Leitch, C.C. Xu, Functionalized wood as bio-based advanced materials: properties, applications, and challenges, Renew. Sustain. Energy Rev. 157 (2022), https://doi.org/10.1016/j.rser.2022.112074.
[8] G.E. Mustoe, Silicification of wood: an overview, Minerals 13 (2023), https://doi.org/10.3390/min13020206.
[9] T. Franke, C. Hinterleitner, A. Maillard, E. Nedelkoska, T. Volkmer, The impact of moisture on salt treated and 2-step mineralized wood, Holzforschung 77 (2023) 541–553, https://doi.org/10.1515/hf-2023-0003.
[10] H.Y. Zhou, D.X. Wen, X.L. Hao, C.F. Chen, N.H. Zhao, R.X. Ou, Q.W. Wang, Nanostructured multifunctional wood hybrids fabricated *via in situ* mineralization of zinc borate in hierarchical wood structures, Chem. Eng. J. 451 (2023), https://doi.org/10.1016/j.cej.2022.138308.
[11] H.Z. Guo, M. Lukovic, M. Mendoza, C.M. Schlepütz, M. Griffa, B.W. Xu, S. Gaan, H. Herrmann, I. Burgert, Bioinspired struvite mineralization for fire-resistant wood, Acs Appl. Mater. Interfaces 11 (2019) 5427–5434, https://doi.org/10.1021/acsami.8b19967.
[12] H.Z. Guo, M. Ozparpucu, E. Windeisen-Holzhauser, C.M. Schleputz, E. Quadranti, S. Gaan, C. Dreimol, I. Burgert, Struvite mineralized wood as sustainable building material: mechanical and combustion behavior, Acs Sustain. Chem. Eng. 8 (2020) 10402–10412, https://doi.org/10.1021/acssuschemeng.0c01769.
[13] V. Merk, M. Chanana, S. Gaan, I. Burgert, Mineralization of wood by calcium carbonate insertion for improved flame retardancy, Holzforschung 70 (2016) 867–876, https://doi.org/10.1515/hf-2015-0228.
[14] V. Merk, M. Chanana, T. Keplinger, S. Gaan, I. Burgert, Hybrid wood materials with improved fire retardance by bio-inspired mineralisation on the nano- and submicron level, Green. Chem. 17 (2015) 1423–1428, https://doi.org/10.1039/c4gc01862a.
[15] A. Pondelak, A.S. Skapin, N. Knez, F. Knez, T. Pazlar, Improving the flame retardancy of wood using an eco-friendly mineralisation process, Green. Chem. 23 (2021) 1130–1135, https://doi.org/10.1039/d0gc03852k.
[16] R. Repic, A. Pondelak, D. Krzisnik, M. Humar, N. Knez, F. Knez, A.S. Skapin, Environmentally friendly protection of European beech against fire and fungal decay using a combination of thermal modification and mineralisation, Wood Mater. Sci. Eng. (2023), https://doi.org/10.1080/17480272.2023.2223508.

[17] J. Huang, J. Liu, S. Lai, D. Liu, Z. Deng, T. Yang, G. Yuan, Enhancing wood fire resistance through magnesium-ion-induced calcium carbonate mineralization, Constr. Build. Mater. 473 (2025) 141069, https://doi.org/10.1016/j.conbuildmat.2025.141069.
[18] D. Mahon, G. Claudio, P. Eames, An experimental study of the decomposition and carbonation of magnesium carbonate for medium temperature thermochemical energy storage, Energies 14 (2021), https://doi.org/10.3390/en14051316.
[19] K.S.P. Karunadasa, C.H. Manoratne, H. Pitawala, R.M.G. Rajapakse, Thermal decomposition of calcium carbonate (calcite polymorph) as examined by in-situ high-temperature X-ray powder diffraction, J. Phys. Chem. Solids 134 (2019) 21–28, https://doi.org/10.1016/j.jpcs.2019.05.023.
[20] R. Rothon, Effects of particulate fillers on flame retardant properties of composites, (2003).
[21] L.A. Hollingbery, T.R. Hull, The thermal decomposition of huntite and hydromagnesite-A review, Thermochim. Acta 509 (2010) 1–11, https://doi.org/10.1016/j.tca.2010.06.012.
[22] V. Choudhary, S. Pataskar, V. Gunjikar, G. ZOPE, Influence of preparation conditions of basic magnesium carbonate on its thermal-analysis, Thermochim. Acta 232 (1994) 95–110.
[23] Y. Sawada, J. Yamaguchi, O. Sakurai, K. Uematsu, N. Mizutani, M. Kato, Thermal decomposition of basic magnesium carbonates under high-pressure gas atmoshpheres, Thermochim. Acta 32 (1979) 277–291.
[24] Y. Sawada, J. Yamaguchi, O. Sakurai, K. Uematsu, N. Mizutani, M. Kato, Thermogravimetric study on the decomposition of hydromagnesite 4MgCO3.Mg(OH)2.4H2O, Thermochim. Acta 33 (1979) 127–140.
[25] C. Padeste, H. Oswald, A. Reller, The thermal-behavior of pure and nickel-doped hydromagnesite in different atmospheres, Mater. Res. Bull. 26 (1991) 1263–1268.
[26] F. Laoutid, P. Gaudon, J. Taulemesse, J. Cuesta, J. Velasco, A. Piechaczyk, Study of hydromagnesite and magnesium hydroxide based fire retardant systems for ethylene-vinyl acetate containing organo-modified montmorillonite, Polym. Degrad. Stab. 91 (2006) 3074–3082, https://doi.org/10.1016/j.polymdegradstab.2006.08.011.
[27] Y.Q. Wu, C.H. Yao, Y.C. Hu, X.D. Zhu, Y. Qing, Q.L. Wu, Comparative performance of three magnesium compounds on thermal degradation behavior of red gum wood, Materials 7 (2014) 637–652, https://doi.org/10.3390/ma7020637.
[28] H. Atay, Novel eco-friendly flame retardant wood composites reinforced by huntite and hydromagnesite minerals, Wood Mater. Sci. Eng. 17 (2022) 648–658, https://doi.org/10.1080/17480272.2021.1923567.
[29] D. Ustaömer, U. Baser, Thermal and fire properties of medium-density fiberboard prepared with huntite/hydromagnesite and zinc borate, Bioresources 15 (2020) 5940–5950.
[30] U.E. Başer, D. Ustaömer, O. Özgenç, Decay Resistance of MDF Manufactured with HuntiteHydromagnesite and Zinc borate, in: Ghent, Belgium, 2017.
[31] A. Pondelak, A. Sever Skapin, N. Knez, R. Repič, L. Škrlep, T. Pazlar, F. Knez, A. Legat, A process of wood mineralization using acetoacetate solutions to improve the essential properties of wood, EP 3 934 869 B1, (2023) 24.
[32] R. Repic, A. Pondelak, D. Krzisnik, M. Humar, A.S. Skapin, Combining mineralisation and thermal modification to improve the fungal durability of selected wood species, J. Clean. Prod. 351 (2022), https://doi.org/10.1016/j.jclepro.2022.131530.
[33] S. Frykstrand, C. Strietzel, J. Forsgren, J. Angstrom, V. Potin, M. Stromme, Synthesis, electron microscopy and X-ray characterization of oxymagnesite, MgO center dot 2MgCO(3), formed from amorphous magnesium carbonate, Crystengcomm 16 (2014) 10837–10844, https://doi.org/10.1039/c4ce01641f.
[34] H. Nguyen, H. Santos, H. Sreenivasan, W. Kunther, V. Carvelli, M. Illikainen, P. Kinnunen, On the carbonation of brucite: Effects of Mg-acetate on the precipitation of hydrated magnesium carbonates in aqueous environment, Cem. Concr. Res. 153 (2022), https://doi.org/10.1016/j.cemconres.2021.106696.
[35] M. Plötze, P. Niemz, Porosity and pore size distribution of different wood types as determined by mercury intrusion porosimetry, Eur. J. Wood Wood Prod. 69 (2011) 649–657, https://doi.org/10.1007/s00107-010-0504-0.
[36] B. Schartel, T.R. Hull, Development of fire-retarded materials - Interpretation of cone calorimeter data, Fire Mater. 31 (2007) 327–354, https://doi.org/10.1002/fam.949.
[37] C. Brischke, G. Alfredsen, Wood-water relationships and their role for wood susceptibility to fungal decay, Appl. Microbiol. Biotechnol. 104 (2020) 3781–3795, https://doi.org/10.1007/s00253-020-10479-1.
[38] H.K. Mustafa, S.S. Anwer, T.J. Zrary, Influence of pH, agitation speed, and temperature on growth of fungi isolated from Koya, Iraq, Kuwait J. Sci. 50 (2023) 657–664.
[39] S.R.M. Ali, A.J. Fradi, A.M. Al-Aaraji, Effect of some physical factors on growth of five fungal species, Eur. Acad. Res. 5 (2017) 1069–1078.
[40] S. Karumuri, S. Hiziroglu, A.K. Kalkan, The distribution and role of nanoclay in lignocellulose-polymer blends, RSC Adv. 7 (2017) 19406–19416, https://doi.org/10.1039/c7ra02082a.
[41] M. Fomina, I. Skorochod, Microbial interaction with clay minerals and its environmental and biotechnological implications, Minerals 10 (2020) 861, https://doi.org/10.3390/min10100861.